Effects of compositional impurities and width variation on the conductance of a quantum wire

1994 J. Phys.: Condens. Matter 6 2559

(http://iopscience.iop.org/0953-8984/6/13/014)

J. Phys.: Condens. Matter 6 (1994) 2559–2572. Printed in the UK

Effects of compositional impurities and width variation on the conductance of a quantum wire

T N Todorov and G A D Briggs
Department of Materials, University of Oxford, Parks Road, Oxford OX1 3PH, UK

Received 19 November 1993

Abstract. An exact single-particle scattering theory formulation of the problem of elastic electronic transport is employed in a 1s tight-binding implementation to study the zero-voltage, zero-temperature conductance of a two-dimensional quantum wire as a function of the Fermi energy. For a perfect wire, the conductance quantization effect is reproduced. Then, the effects on the conductance of compositional impurities and width variation in the wire are studied. It is found that the quantization effect is seriously damaged even with minimal amounts of impurity, whereas it exhibits some tolerance towards width variation, especially at low carrier concentrations. It is found that with both types of disorder the conductance is particularly strongly suppressed at Fermi energies close to the edges of the subbands for the perfect wire, which, in agreement with previous findings, shows that at those energies the localization of the electrons by the disorder is enhanced.

1. Introduction

Recent advances in semiconductor technology have made it possible to manufacture a variety of pseudo two- and one-dimensional structures. A particular kind, often referred to as quantum wires, are long and narrow strips of conducting material. The problem of electronic transport in quantum wires in the elastic (phonon-free) regime has attracted intense attention due to the presence of an interesting quantum effect, namely the quantization of the zero-voltage, zero-temperature DC conductance of the perfect wire, as a function either of the wire width or of the position of the Fermi energy (or, equivalently, of the electron density).

This effect, which has a well understood origin [1, 2, 3, 4, 5, 6, 7, 8] and of which there have recently been clear experimental observations in nearly perfect long and narrow quantum wires [9], is due to the quantization of the transverse momentum quantum number in the wire. With each value of the quantized transverse momentum is associated a subband of current-carrying electronic states, each subband contributes one quantum unit of conductance, $e^2/\pi\hbar$, and the conductance is simply given by $Ne^2/\pi\hbar$, where N is the number of subbands available at the Fermi energy.

However, a perfect quantum wire is difficult to make and therefore it is essential (and also interesting) to assess the effects of defects, such as compositional impurity or geometric imperfections, on the transport characteristics of the wire. The zero-voltage, zero-temperature conductance of a wire containing a single scatterer [10] and of a wire with a single smooth widening in the shape of a 'swelling' [11] have recently been investigated and in both cases it is found that the quantization of the conductance is damaged or fully destroyed. Recently, there have also been two studies [12, 13], in a 1s tight-binding model, of the effects of random impurity contamination and width variation on the density of states

0953-8984/94/132559+14$19.50

and on the localization length of the electronic states in a wire of thickness of up to several atomic layers. It is found that the density of states is altered relative to what it is in the perfect wire, which suggests that the quantization of the conductance would be damaged or lost, and that the disorder in the wire leads to finite localization lengths, which suggests that the conductance would be suppressed relative to the perfect case.

The present paper contains a study of the effects of impurity contamination and of width variation directly on the zero-voltage, zero-temperature, elastic DC conductance of a quantum wire. The calculation employs an orthonormal 1s tight-binding model [12, 13, 14] and is based on an exact single-particle scattering theory formulation of the problem of elastic quantum transport, developed and discussed elsewhere [15].

2. Calculation of the conductance

The general geometry, the conductance of which is to be calculated, is presented in figure 1. The quantum wire connects two semi-infinite perfect two-dimensional crystals. The wire and the crystals all have the same simple square lattice structure of lattice parameter a. The wire can be viewed as an array in the x-direction of one-dimensional atomic layers, each of which lies in the y-direction. The number N of such layers specifies the length of the wire. The width W of the wire, on the other hand, is defined as the number of atoms in a given layer. W may vary along the length of the wire. The electronic structure of the system is approximated by an orthonormal nearest-neighbour 1s tight-binding model with a nearest-neighbour hopping integral γ and an on-site energy on the native atoms of zero.

The calculation of the conductance requires some preliminary work, which will be described next.

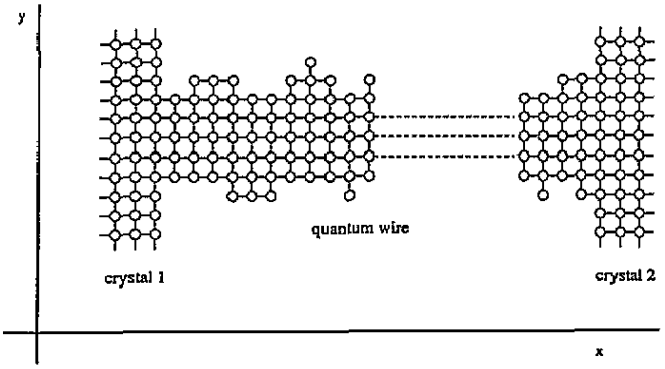

Figure 1. The quantum wire geometry. The quantum wire connects the two semi-infinite crystals 1 and 2. The entire system has a two-dimensional simple square lattice geometry with a lattice constant a. The length of the wire N is defined as the number of atomic layers of the wire. The width of the wire W is defined as the number of atoms in a given wire layer. The nearest-neighbour hopping integrals are all equal to γ and are indicated by the lines joining the atoms. This geometry will be used as the 'final situation' in the calculation of the conductance.

2.1. The surface Green function for the bare semi-infinite simple square lattice

Consider only the semi-infinite simple square crystal 1 from figure 1 (i.e., imagine that the wire and crystal 2 are not there). We will require the matrix elements of its retarded Green function between surface atomic sites. The general method, used in this work for

calculating such matrix elements, has been described in detail in [15] and therefore here it will be sketched only briefly, for completeness.

The semi-infinite simple square lattice can be regarded as an array in the x-direction of infinite one-dimensional atomic chains, lying in the y-direction. Let us number them from 1 to ∞ with chain 1 being the surface chain. Each atomic chain in isolation has a set of eigenstates $\{|K\rangle\}$ given by

$$|K\rangle = \frac{1}{\sqrt{N_1}} \sum_n \exp(inK)\,|n\rangle \tag{1}$$

where N_1 is the number of atoms in the chain with $N_1 \to \infty$, $|n\rangle$ is the 1s state on the nth chain atom and $K = ka$ with k being the wave-vector along the chain. The chain states $\{|K\rangle\}$ have energies $\{\mathcal{E}(K)\}$, in units of $|\gamma|$, given by

$$\mathcal{E}(K) = -2\cos(K) \tag{2}$$

where $K \in [-\pi, \pi]$. Let now $\{|l, K\rangle\}$ be the chain states for the lth chain in the semi-infinite simple square lattice. If H is the Hamiltonian for the lattice, we have that the matrix element $\langle l, K|H|m, K'\rangle$ is not identically equal to zero only if $K = K'$. For the case $K = K'$, we denote the above matrix element by $H_{lm}(K)$ and note that if $l = m$, then $H_{lm}(K) = |\gamma|\mathcal{E}(K)$; if $l = m \pm 1$, then $H_{lm}(K) = \gamma$ and finally, if $l \neq m$ and $l \neq m \pm 1$, then $H_{lm}(K) = 0$.

Since H is diagonal in the label K, so will be $G^{0+}(E)$, where $G^{0+}(E)$ is the retarded Green function for the lattice. Let us write $G^{0+}_{lm}(E, K)$ for the matrix element $\langle l, K|G^{0+}(E)|m, K\rangle$. Consider now appending another chain to the end of the semi-infinite lattice. Let this chain have index 0. Let its bonding to the rest of the lattice be realized by a term V in the Hamiltonian, so that the only non-zero matrix elements of V, in the basis of the chain states $\{|l, K\rangle\}$, are $V_{01}(K) = V_{10}(K) = \gamma$. We also have $G^{0+}_{00}(E, K) = 1/(E - |\gamma|\mathcal{E}(K) + i\epsilon)$, where $\epsilon \to 0^+$, and $G^{0+}_{0n}(E, K) = G^{0+}_{n0}(E, K) = 0$ for all $n \neq 0$. Let $G^+(E)$ be the retarded Green function for the lattice with the new chain bonded to it. Solving the Dyson equation

$$G^+(E) = G^{0+}(E) + G^{0+}(E)VG^+(E) \tag{3}$$

we easily obtain

$$G^+_{00}(E, K) = \frac{1}{|\gamma|} \frac{\mathcal{E} - \mathcal{E}(K) \pm \sqrt{[\mathcal{E} - \mathcal{E}(K)]^2 - 4}}{2} \tag{4}$$

where $\mathcal{E} = E/|\gamma|$ and we choose the solution with the minus sign if the expression under the square root is negative, while if this expression is positive, we choose the solution with the minus sign if $[\mathcal{E} - \mathcal{E}(K)] > 0$ and the solution with the plus sign if $[\mathcal{E} - \mathcal{E}(K)] < 0$. (The rules for choosing between the two solutions are discussed in [15].)

Consider now two atomic sites, p and q, on the surface of the semi-infinite lattice. Let them be n lattice parameters apart. Consider the matrix element of $G^+(E)$ between them. Call this matrix element $G^+(E, n)$. We have

$$G^+(E, n) = \langle p|G^+(E)|q\rangle = \sum_{l,m,K} \langle p|l, K\rangle G^+_{lm}(E, K)\langle m, K|q\rangle$$

$$= \frac{1}{N_1} \sum_K \exp(inK)\, G^+_{00}(E, K). \tag{5}$$

Finally, replacing $(1/N_1)\sum_K$ by $(1/2\pi)\int_{-\pi}^{\pi} dK$ we obtain

$$G^+(E, n) = \frac{1}{2\pi} \int_{-\pi}^{\pi} \cos(nK)\, G^+_{00}(E, K)\, dK \tag{6}$$

where in replacing $\exp(inK)$ by $\cos(nK)$ we have made use of the fact that $G_{00}^{+}(E, K)$ is an even function of K. The desired Green function matrix elements between surface sites of the semi-infinite simple square lattice can be obtained from equation (6), after substituting for $G_{00}^{+}(E, K)$ from equation (4). The integration in (6) is performed numerically.

2.2. *Growth of the quantum wire*

The next stage in the calculation of the conductance of the geometry from figure 1 consists in growing the wire [16], layer by layer, on crystal 1. In the first step of the growth sequence (figure 2(a)), the first atomic layer of the wire is bonded to the surface of crystal 1, in the second growth step, the second layer of the wire is bonded to the first layer, and so on.

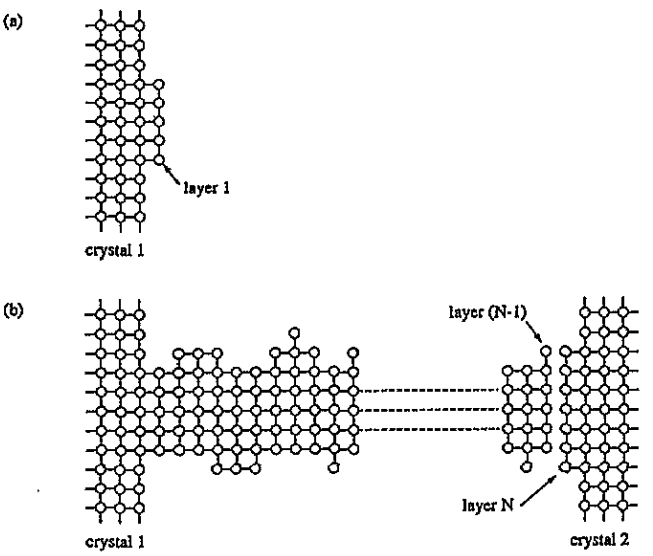

Figure 2. (a) The geometry after the first step in the growth of the wire. (b) The geometry at the end of the growth sequence. Notice that there still is no bonding between layers $(N-1)$ and N of the wire. This geometry will be used as the 'initial situation' in the calculation of the conductance.

At every step of the growth sequence, the retarded Green function matrix elements between atomic sites in the last added layer are calculated by writing the Dyson equation, (3), as

$$[1 - G^{0+}(E)V]G^{+}(E) = G^{0+}(E) \tag{7}$$

and solving it numerically. For a typical growth step, say growth step k with $k > 1$, the quantitites $G^{0+}(E)$, V and $G^{+}(E)$ are constructed as follows.

$G^{0+}(E)$ is the Green function for the situation just before the growth step. In this situation the wire has been grown up to and including layer $(k-1)$, whereas the atoms in layer k are not bonded to each other or to the atoms in layer $(k-1)$. The matrix elements of $G^{0+}(E)$ between atoms within layer $(k-1)$ are available from the previous growth step, those between an atom in layer $(k-1)$ and an atom in layer k or between two different atoms within layer k are all zero, while the on-site matrix element of $G^{0+}(E)$ on an atom in layer k is given by $1/(E - E_a + i\epsilon)$, where E_a is the on-site energy on the atom and $\epsilon \to 0^{+}$.

The term V describes the bonding of the atoms in layer k to each other and to the atoms in layer $(k-1)$. Thus, the matrix element of V between two atoms in layer k or between an atom in layer k and an atom in layer $(k-1)$ is equal to γ if the atoms are nearest neighbours and is zero otherwise. All other matrix elements of V are zero.

$G^+(E)$ is the Green function for the situation just after the kth growth step, when the wire is grown up to and including layer k.

In the case of the first growth step, $G^{0+}(E)$, V and $G^+(E)$ are constructed in the same way, except that in the situation before the growth step (i.e., the situation described by $G^{0+}(E)$), no part of the wire has been grown yet and we have the bare crystal 1 plus the decoupled atoms of the first wire layer.

The growth sequence is continued up to and including layer $(N-1)$ of the wire. The Nth layer of the wire is then bonded to the surface of crystal 2. This situation (figure 2(b)), in which there still is no bonding (hopping integrals) between layers $(N-1)$ and N of the wire, will be used in the calculation of the conductance.

2.3. *The conductance*

The geometry from figure 2(b), which below will be referred to as the 'initial situation', consists of two decoupled semi-infinite systems: one of them, system 1, is crystal 1 with the wire up to and including layer $(N-1)$ grown on it, and the other one, system 2, is crystal 2 with layer N of the wire bonded to it. Let $G^{0+}(E)$ now be the retarded Green function for the initial situation. The matrix elements of $G^{0+}(E)$ between atoms within layer $(N-1)$ and those between atoms within layer N are available from the growth sequence, while those between an atom in layer $(N-1)$ and an atom in layer N are all zero. Let us introduce $G_1^{0+}(E)$ and $G_2^{0+}(E)$ as the projections of $G^{0+}(E)$ on to systems 1 and 2 respectively. Thus, if p and q are two atomic sites, we have that the matrix element $\langle p|G_1^{0+}(E)|q\rangle$ is equal to $\langle p|G^{0+}(E)|q\rangle$ if both p and q are in system 1, and is zero otherwise, and analogously for the matrix elements of $G_2^{0+}(E)$. Let $\rho_1^0(E)$ and $\rho_2^0(E)$ be the density of states operators for systems 1 and 2 respectively, given by

$$\rho_j^0(E) = \frac{1}{2\pi i}[G_j^{0-}(E) - G_j^{0+}(E)] \qquad j = 1, 2 \tag{8}$$

where $G_j^{0-}(E) = [G_j^{0+}(E)]^\dagger$.

In the geometry from figure 1, which below will be referred to as the 'final situation', systems 1 and 2 are fully bonded to form a single infinite system. Let $G^+(E)$ be the retarded Green function for the final situation.

The transition from the initial to the final situation is realised by the addition to the initial Hamiltonian of a term V, containing the hopping integrals between systems 1 and 2. Thus, the only non-zero matrix elements of V are of the form $V_{12} = V_{21} = \gamma$, where indices 1 and 2 designate an atom in layer $(N-1)$ and its nearest neighbour in layer N of the wire, respectively.

As is proved in [15], the zero-voltage, zero-temperature elastic conductance g of the geometry in the final situation is given by

$$g = \frac{e^2}{\pi\hbar} 4\pi^2 \operatorname{Tr}[\rho_1^0(E_F)t^\dagger(E_F)\rho_2^0(E_F)t(E_F)] \tag{9}$$

where E_F is the absolute position of the Fermi energy and the operator $t(E)$ is given by

$$t(E) = V + VG^+(E)V. \tag{10}$$

Using the Dyson equation for $G^+(E)$, (3), one can write equation (10) as

$$[1 - VG^{0+}(E)]t(E) = V. \tag{11}$$

The conductance g is found by taking the trace in equation (9) in the orthonormal atomic basis after solving equation (11) numerically to find the respective matrix elements of $t(E_F)$.

3. Results and discussion

The dispersion relation for the 1s band for the two-dimensional simple square lattice with zero on-site energies is

$$\mathcal{E} = -2\cos(K_x) - 2\cos(K_y) \tag{12}$$

where $\mathcal{E}$ is the band energy in units of $|\gamma|$ and $K_{x,y} = k_{x,y}a$ with $k = (k_x, k_y)$ being the wave-vector in the plane of the lattice. The first Brillouin zone is given by $|K_{x,y}| \in [0, \pi]$. Thus, the 1s band energy $\mathcal{E}$ lies in the interval $[-4, 4]$. The band is half-filled for $\mathcal{E}_F = 0$, where $\mathcal{E}_F = E_F/|\gamma|$.

In the present work, the conductance g for a given wire is calculated as a function of $\mathcal{E}_F$ for values of $\mathcal{E}_F$ lying in the interval $[-4, 4]$ and spaced by 0.01.

3.1. The perfect wire

First we consider the case of a perfect wire, defined as a wire of uniform width W and straight edges (i.e., not a meandering wire of constant width), and with on-site energies equal to zero as in the two semi-infinite crystals 1 and 2 (figure 3). Figure 4 contains plots of g (in units of $e^2/\pi\hbar$) versus $\mathcal{E}_F$ for a wire of length $N = 10$ and width $W = 10$ (lower curve) and for a wire of length $N = 100$ and width $W = 10$ (upper curve). The two curves are offset by unity in the vertical direction. The gross structure of the curves consists of sharp unit conductance steps (in units of $e^2/\pi\hbar$). The fine structure of the curves consists of ripples, superimposed on the sharp steps.

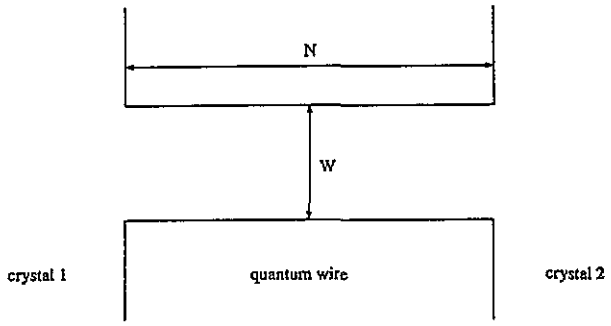

Figure 3. The geometry with a perfect wire of length N and width W.

In a 1s tight-binding model, a perfect two-dimensional wire with a simple square lattice geometry and of width W atoms has W subbands, defined by $K_y = K_y(n) = n\pi/(W + 1)$, $n = 1, 2, ..., W$. The bottom of the nth subband corresponds to $K_x = 0$, $K_y = K_y(n)$ and therefore, from the dispersion relation (12), lies at an energy, in units of $|\gamma|$, of $-2 - 2\cos[K_y(n)]$. The top of the nth subband corresponds to $K_x = \pi$, $K_y = K_y(n)$ and lies at an energy, in units of $|\gamma|$, of $+2 - 2\cos[K_y(n)]$. As may easily be verified,

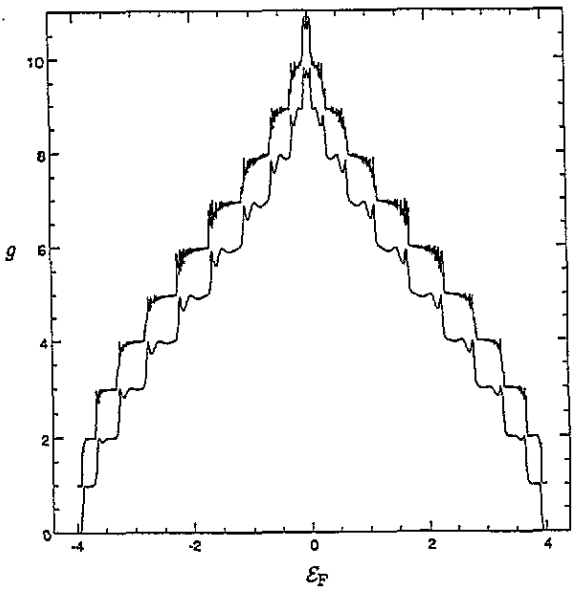

Figure 4. Plots of the conductance g in units of $e^2/\pi\hbar$ versus the Fermi energy in units of $|\gamma|$, $\mathcal{E}_F$, for a perfect wire of length $N = 10$ and width $W = 10$ (lower curve) and for a perfect wire of length $N = 100$ and width $W = 10$ (upper curve). The two curves are offset by unity in the vertical direction.

the bottoms of the ten subbands for the case $W = 10$ coincide with the values of $\mathcal{E}_F$ at which in figure 4 we see jump-like increases in the conductance, while the tops of the ten subbands coincide with the values of $\mathcal{E}_F$ at which in figure 4 we see jump-like decreases in the conductance. Therefore, the gross structure of the g versus $\mathcal{E}_F$ curves corresponds to the opening and closing of conduction channels, which correspond to the various subbands for the perfect wire. Each conduction channel contributes one quantum unit of conductance $(e^2/\pi\hbar)$ and the conductance of the perfect wire is thus quantized.

The fine structure of the curves, namely the ripples, also known as 'ringing' [16], is due to the multiple reflections at the interfaces between the wire and the semi-infinite crystals. For certain values of $\mathcal{E}_F$, K_x in one or more of the available subbands is such that the Fermi electrons in these subbands can form quasi-standing waves in the wire region. These electrons thus become partially trapped in the wire and the conductance undergoes a slight depression. The amount of ringing is reduced by reducing the ratio of the length of the wire to its width, which can be seen by comparing the two curves in figure 4.

The symmetry about the point $\mathcal{E}_F$ of the two curves is due to the combination between the symmetry about the same point of the 1s bands for crystals 1 and 2, and the fact that the on-site energies in the wire itself are all equal to zero.

The results for the perfect wire will be used now as the basis for investigating the effects of compositional impurity and width variation on the conductance of the wire.

3.2. Compositional impurity

In the study of the effects of impurity contamination on the conductance, we once again consider wires of uniform width and straight edges. All nearest-neighbour hopping integrals are equal to γ as before, but now the on-site energy on randomly selected wire atoms is

made different from the native on-site energy of zero. Thus, a particular impure wire is defined by its length N, its uniform width W, the percentage p and the on-site energy $\mathcal{E}_{\text{imp}}$ (in units of $|\gamma|$) of the impurity atoms.

Figure 5 contains a plot of g (in units of $e^2/\pi\hbar$) versus $\mathcal{E}_{\text{F}}$ for the wire of length $N = 100$ and width $W = 10$ with impurity contamination with $p = 3\%$ and $\mathcal{E}_{\text{imp}} = -1$ (lower curve). The curve for the same wire without the impurities is also shown for comparison (upper curve). The two curves are offset by unity in the vertical direction. Even though with $p = 3\%$ there would only be about 30 impurity atoms in this wire of 1000 atoms, the shape of the conductance curve has been damaged strongly. There is only a faint trace of the conductance steps, the curve is highly irregular and the conductance is suppressed relative to the case of the perfect wire. The loss of the conductance quantization effect and the overall irregularity of the curve are due to the destruction of the periodicity of the wire (and hence of the subband structure, present in the perfect wire). The suppression of the conductance, on the other hand, is due to the back-scattering introduced by the impurity atoms. Observe also that the symmetry of the conductance curve about the point $\mathcal{E}_{\text{F}} = 0$ has been broken. This is due to the presence in the wire of atoms with non-zero on-site energies.

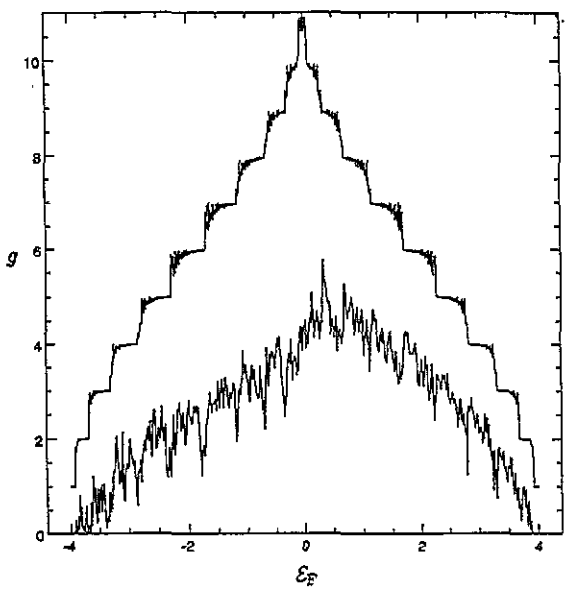

Figure 5. A plot of the conductance g in units of $e^2/\pi\hbar$ versus $\mathcal{E}_{\text{F}}$ for the wire of length $N = 100$ and width $W = 10$ with impurity contamination with $p = 3\%$ and $\mathcal{E}_{\text{imp}} = -1$ (lower curve). The curve for the same wire without the impurities is also shown for comparison (upper curve). The two curves are offset by unity in the vertical direction.

A prominent feature of the curve for the impure wire is the marked conductance minima around the values of $\mathcal{E}_{\text{F}}$ at which in the case of the perfect wire we see quantized conductance jumps, or in other words, in the vicinity of the perfect wire subband edges. A similar effect has been found in a study of the conductance of a wire containing a single scatterer [10]. Likewise, in the calculations in [13] minima around the subband edges are found in the electron *localization length* in geometrically perfect but compositionally impure two-dimensional wires.

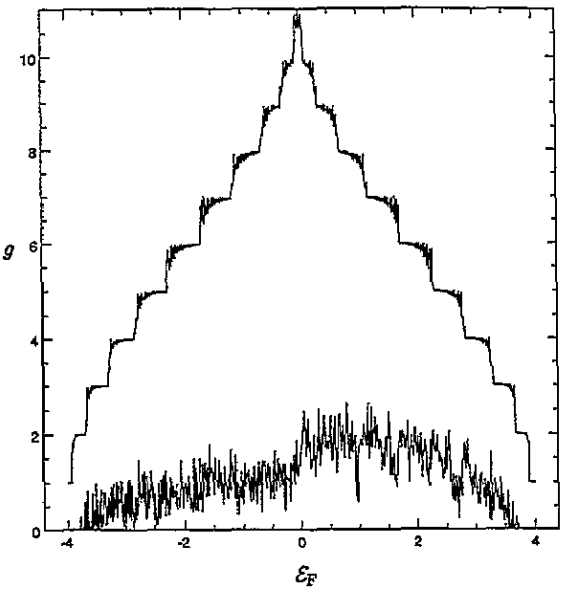

Figure 6. A plot of the conductance g in units of $e^2/\pi\hbar$ versus $\mathcal{E}_F$ for the wire of length $N = 100$ and width $W = 10$ with impurity contamination with $p = 15\%$ and $\mathcal{E}_{imp} = -1$ (lower curve). The curve for the same wire without the impurities is also shown for comparison (upper curve). The two curves are offset by unity in the vertical direction.

Increasing the percentage of the impurity atoms to $p = 15\%$ (figure 6) leads to a complete disappearance of the conductance steps and to a very significant suppression of the conductance. Notice also the slight shift of the entire g versus $\mathcal{E}_F$ curve in the negative $\mathcal{E}_F$ direction. This effect is due to the lowering of the *average* on-site energy in the wire.

3.3. Width variation

Now we turn to the effect on the conductance of variation in the width (also called surface roughness) of the quantum wire. We consider a wire of total length N without any impurities. The wire has alternating narrow and wide regions of widths, in numbers of atoms, W_1 and W_2 respectively. One edge of the wire is smooth so the variation in the width of the wire manifests itself as roughness along the other edge. The length in the x-direction of each region, in numbers of wire layers, is $(L_{cor} - L_{var})$, L_{cor}, or $(L_{cor} + L_{var})$ with a probability of $\frac{1}{3}$ in each case. L_{cor} is the correlation length of the roughness and L_{var} is a measure of the variation about L_{cor} of the length of a typical narrow or wide region. The above geometry is shown in figure 7.

Figure 8 contains a plot of the conductance g (in units of $e^2/\pi\hbar$) versus $\mathcal{E}_F$ for a rough wire with $N = 100$, $W_1 = 10$, $W_2 = 11$, $L_{cor} = 10$ and $L_{var} = 1$ (lowermost curve). The curves for the perfect wire with $N = 100$, $W = W_1 = 10$ (middle curve) and for the perfect wire with $N = 100$, $W = W_2 = 11$ (uppermost curve) are also shown for comparison. Each pair of neighbouring curves are offset by unity in the vertical direction. Unlike the impurity curves, the curve for the rough wire has well marked conductance steps. Moreover, both in their number and in their positions, these steps correspond more closely to those found in the case of the perfect wire with $W = W_1 = 10$ than to those found in the case of the perfect wire with $W = W_2 = 11$. Thus, a rough wire of narrow and wide regions of

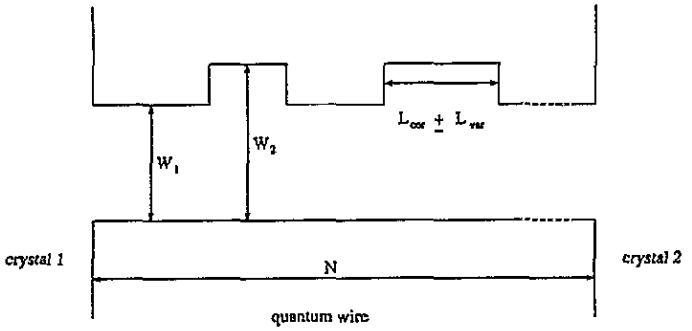

Figure 7. The geometry for the width variation calculation. The wire has alternating narrow and wide regions of widths W_1 and W_2 respectively. The length of each region is $(L_{cor} - L_{var})$, L_{cor}, or $(L_{cor} + L_{var})$ with a probability of $\frac{1}{3}$ in each case.

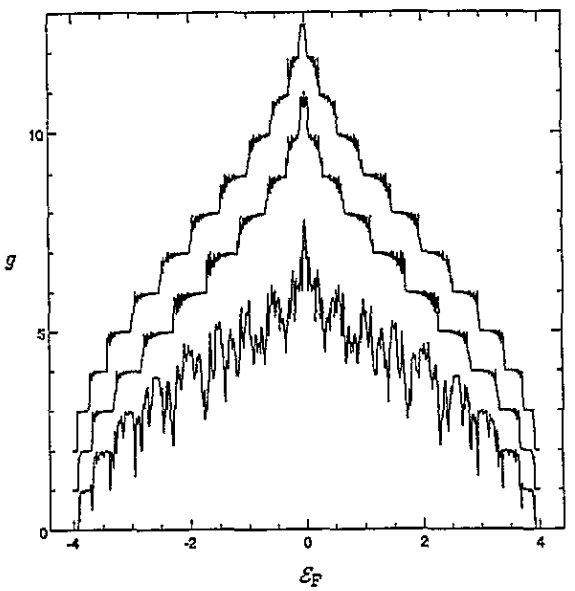

Figure 8. A plot of the conductance g in units of $e^2/\pi\hbar$ versus $\mathcal{E}_F$ for a rough wire with $N = 100$, $W_1 = 10$, $W_2 = 11$, $L_{cor} = 10$ and $L_{var} = 1$ (lowermost curve). The curves for the perfect wire with $N = 100$, $W = W_1 = 10$ (middle curve) and for the perfect wire with $N = 100$, $W = W_2 = 11$ (uppermost curve) are also shown for comparison. Each pair of neighbouring curves is offset by unity in the vertical direction.

widths W_1 and W_2, respectively, 'perceives' itself as a perturbed version of a perfect wire of width W_1 rather than as a perturbed version of a perfect wire of width W_2. For this reason in the rest of the discussion the conductance of such a rough wire will be related to and compared with the conductance and the underlying subband structure of the corresponding perfect wire of width W_1. The first two or three conductance steps in the rough case are more or less square in shape and have the size of the quantum unit, as in the perfect case. The higher-order steps have an increasingly more ragged appearance and smaller height. This means that, as may be expected, the effect of width variation on the electronic states in the wire is weakest for states in the subbands with the lowest values of the transverse

wave-vector K_y.

The conductance for the rough wire has pronounced minima around those energies at which the conductance for the perfect wire undergoes quantized jumps, indicating that exactly as in the case of impurity contamination, the propagation of electronic states with energies close to the subband edges is impeded particularly effectively by the disorder. Observe also that with all on-site energies being zero, the conductance curve for the rough wire is symmetric about the point $\mathcal{E}_F$.

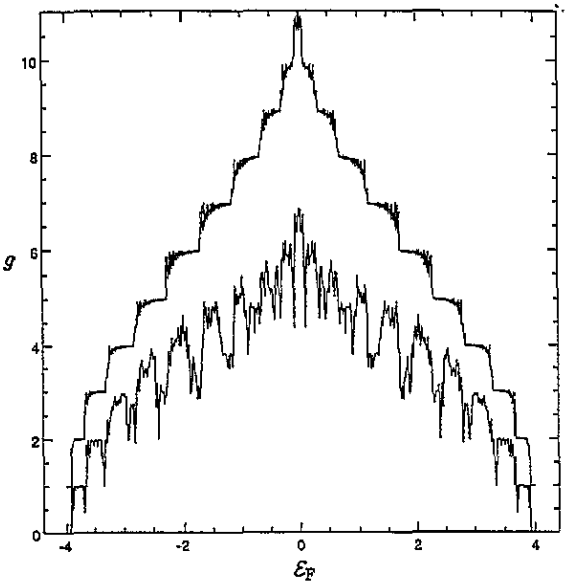

Figure 9. A plot of the conductance g in units of $e^2/\pi\hbar$ versus $\mathcal{E}_F$ for a rough wire with $N = 100$, $W_1 = 10$, $W_2 = 11$, $L_{cor} = 10$ and $L_{var} = 3$ (lower curve). The curve for the perfect wire with $N = 100$, $W = W_1 = 10$ is also shown for comparison (upper curve). The two curves are offset by unity in the vertical direction.

Increasing L_{var} to three (figure 9) does not alter much the appearance of the conductance steps or the size of the conductance, but causes the conductance minima near the subband edges to become more prominent. Increasing the amplitude, $(W_2 - W_1)$, of the width variation in the wire, on the other hand, affects the conductance steps strongly and suppresses the conductance, as may be seen from figure 10, which contains the results for the case $N = 100$, $W_1 = 10$, $W_2 = 12$, $L_{cor} = 10$, $L_{var} = 1$.

The effect of varying L_{cor} is quantitative rather than qualitative. Figure 11 contains the conductance curve for the case $N = 100$, $W_1 = 10$, $W_2 = 11$, $L_{cor} = 5$, $L_{var} = 1$. As may be seen from a comparison with figure 8, the conductance is reduced relative to the case $L_{cor} = 10$. This is due to the increase, with decreasing L_{cor}, in the scattering per unit length of the wire. The reduction in L_{cor} leads also to a widening of the conductance minima near the subband edges.

In the past, in continuum (as opposed to tight-binding) studies of the electron *mobility* as a function of the correlation length of smooth width variation in narrow two-dimensional regions, at a fixed Fermi energy, chosen such that there is only one available subband, it has been found [17, 18] that the mobility goes through a minimum when the correlation length of the roughness becomes comparable to the Fermi wavelength. One might expect

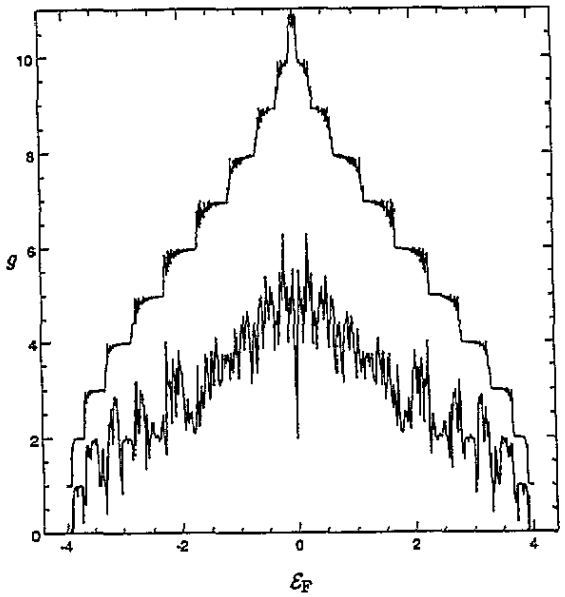

Figure 10. A plot of the conductance g in units of $e^2/\pi\hbar$ versus $\mathcal{E}_F$ for a rough wire with $N = 100$, $W_1 = 10$, $W_2 = 12$, $L_{cor} = 10$ and $L_{var} = 1$ (lower curve). The curve for the perfect wire with $N = 100$, $W = W_1 = 10$ is also shown for comparison (upper curve). The two curves are offset by unity in the vertical direction.

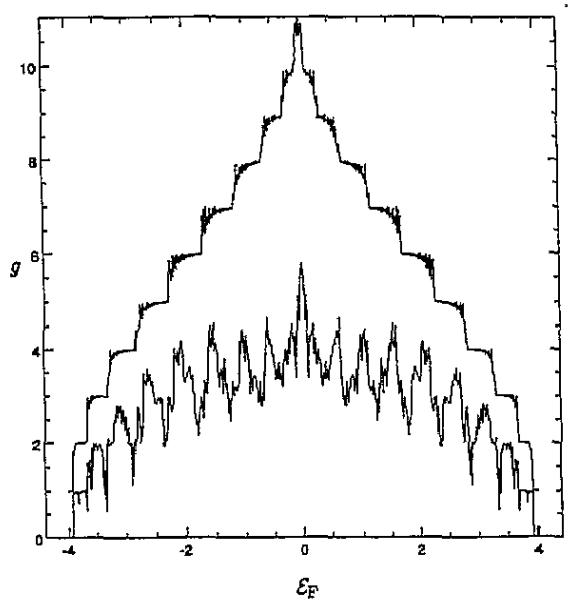

Figure 11. A plot of the conductance g in units of $e^2/\pi\hbar$ versus $\mathcal{E}_F$ for a rough wire with $N = 100$, $W_1 = 10$, $W_2 = 11$, $L_{cor} = 5$ and $L_{var} = 1$ (lower curve). The curve for the perfect wire with $N = 100$, $W = W_1 = 10$ is also shown for comparison (upper curve). The two curves are offset by unity in the vertical direction.

by analogy that in the present roughness calculations the conductance would have local

minima at those values of $\mathcal{E}_F$ at which in one of the available subbands $2\pi/K_x$ becomes similar to L_{cor}, thereby enabling the Fermi electrons to form quasi-standing waves in the narrow and wide regions of the wire. However, even though it should exist in principle, in the present set-up this effect cannot be seen, because it has the same mechanism and therefore the same size as the 'ringing' phenomenon, and is thus masked by the latter.

4. Concluding remarks

The purpose of the present calculations is to provide a visual quantitative picture of the effects of compositional impurities and width variation *directly on the conductance* of a quantum wire.

The calculations on the perfect wires illustrate the manifestation and the mechanism of the conductance quantization effect and show an interesting consequence of the chosen geometry, namely the fine conductance oscillations, or ringing, that are due to partial electron trapping by the formation of quasi-standing waves in the wire and which, by their very nature, may be clearly observed only in the phonon-free regime.

The calculations on wires with compositional impurity or non-uniform width give an idea of how good a quantum wire must be for the quantization effect to be at least partially preserved.

Qualitatively, impurity contamination and width variation have the same effect of suppressing the conductance and of damaging or destroying the conductance quantization. With both types of disorder there is enhanced suppression of the conductance at Fermi energies close to the subband edges. This is a direct manifestation of the previously established result that the electron *localization length* has local minima at these energies.

The essential quantitative result of this study is that destruction of the conductance quantization and strong suppression of the conductance are achieved even with minimal amounts of impurities in the wire, while with small-amplitude width variation the quantization effect survives partially. In fact, while the destructive effect of impurity contamination on the conductance quantization is more or less uniform throughout the conduction band, in the case of width variation, the conductance steps at low $\mathcal{E}_F$ (which correspond to the opening of the subbands with the lowest values of the transverse wavevector) suffer relatively slight damage. Therefore, the effects of surface roughness in a real wire may be partially overcome by adjusting the Fermi level in the wire, whereas the effects of impurity contamination, in addition to being more drastic, would plague one at all carrier concentrations.

Acknowledgments

Financial support from the St Cyril and Methodius International Foundation, the Worshipful Company of Ironmongers, Smith Associates, the Edward Boyle Memorial Trust and Oxford University is gratefully acknowledged. The authors also wish to thank Dr A P Sutton, A T Michels, Professor B A Joyce and Professor A C Gossard for interesting and fruitful discussions.

References

[1] van der Marel D and Haanappel E G 1989 *Phys. Rev.* B **39** 7811
[2] Szafer A and Stone A D 1989 *Phys. Rev. Lett.* **62** 300
[3] Escapa L and Garcia N 1989 *J. Phys.: Condens. Matter* **1** 2125

[4] Glazman L I, Lesovik G B, Khmelnitskii D E and Shekhter R I 1988 *JETP Lett.* **48** 239
[5] Streda P 1989 *J. Phys.: Condens. Matter* **1** 1025
[6] Escapa L and Garcia N 1990 *Appl. Phys. Lett.* **56** 901
[7] Nixon J A and Davies J H 1991 *Phys. Rev.* B **43** 12 638
[8] Sone J 1992 *Semicond. Sci. Technol.* **7** B210
[9] Ismail K, Washburn S and Lee K Y 1991 *Appl. Phys. Lett.* **59** 1998
[10] Kunze Ch and Lenk R 1992 *Solid State Communi.* **84** 457
[11] Yuan S-q and Gu B-y 1993 *Z. Phys.* B **92** 47
[12] Taylor J P G, Hugill K J, Vvedensky D D and MacKinnon A 1991 *Phys. Rev. Lett.* **67** 2359
[13] Nikolic K and MacKinnon A 1993 *Phys. Rev.* B **47** 6555
[14] Sutton A P, Finnis M W, Pettifor D G and Ohta Y 1988 *J. Phys. C: Solid State Phys.* **21** 35
[15] Todorov T N, Briggs G A D and Sutton A P 1993 *J. Phys.: Condens. Matter* **5** 2389
[16] Pendry J B, Prêtre A B, Rous P J and Matrin-Moreno L 1991 *Surf. Sci.* **244** 160
[17] Sakaki H, Noda T, Hirakawa K, Tanaka M and Matsusue T 1987 *Appl. Phys. Lett.* **51** 1934
[18] Motohisa J and Sakaki H 1992 *Appl. Phys. Lett.* **60** 1315